Two-component System CCl_4 + $(CH_3)_3CBr$: Extrema in Equilibria Involving Orientationally Disordered Phases

M. Barrio,[†] L. C. Pardo,[†,‡] J. Ll. Tamarit,*[,†] Ph. Negrier,[§] J. Salud,[†] D. O. López,[†] and D. Mondieig[§]

Departament de Física i Enginyeria Nuclear, E.T.S.E.I.B. Universitat Politècnica de Catalunya, Diagonal, 647 08028 Barcelona, Catalonia, Spain, Experimental Physics V, Center for Electronic Correlations and Magnetism, University of Augsburg, 86135 Augsburg, Germany, and Centre de Physique Moléculaire, Optique et Hertzienne, UMR 5798 au CNRS-Université Bordeaux I, 351, cours de la Libération, 33405 Talence Cedex, France

Received: March 10, 2006; In Final Form: April 26, 2006

Phase equilibria involving orientationally disordered (OD) and liquid phases of the two-component system between carbon tetrachloride (CCl_4) and 2-methyl-2-bromomethane ($(CH_3)_3CBr$) have been determined by means of X-ray powder diffraction and thermal analysis techniques from 210 K up to the liquid state. The isomorphism relation between the OD stable face-centered cubic (FCC) phase of $(CH_3)_3CBr$ and the metastable FCC phase of CCl_4 has been demonstrated throughout the continuous evolution of the lattice parameters and the existence of the two-phase equilibrium [FCC + L] for the whole range of composition, despite the monotropy of the FCC phase for the CCl_4 component with respect to its OD rhombohedral (R) stable phase. A continuous series of OD R mixed crystals is found, which confirms the R lattice symmetry of the OD phase II of $(CH_3)_3CBr$, for which the crystallographic results have been long-time misinterpreted. X-ray patterns of such a phase were indexed according to the recent single-crystal results obtained by Rudman (Rudman, R. *J. Mol. Struct.* **2001**, *569,* 157). In addition, some experimental evidences are given to confirm the number of molecules per unit cell ($Z = 21$). The thermodynamic assessment reproduces coherently the phase diagram for the stable [R + L] and [R + FCC] two-phase equilibria as well as for the partially metastable [FCC + L] two-phase equilibrium and provides a set of data for the thermodynamic properties of nonexperimentally available phase transitions of pure components. Surprisingly, the phase equilibrium involving R and FCC OD phases appears as one of the very few showing a solid−solid equilibrium with two extremes.

Introduction

Substances whose molecular shapes are symmetrical about one or more axes and, particularly, those where the molecular shape is somewhat globular, have been found to show a rich polymorphism.[1−5] At temperatures below melting, that is, in the solid state, these molecules possess at least one phase characterized by a dynamic orientational disorder with a more or less restricted rotational freedom. Such solid phases are commonly referred to as plastic phases or orientationally disordered (OD) crystals.[1−6] Well-known examples of such materials are the *tert*-butyl compounds, $(CH_3)_3CX$, X═Cl, Br, NO_2, CN, SH, ..., because they have molecular shapes sufficiently close to spherical (due to the comparable size of the X groups) to enable orientational disorder in the solid state.[3,5,6]

tert-Butyl compounds have stimulated a large number of theoretical studies as well as have been the object of considerable experimental efforts to elucidate the nature of the disorder and, more specifically, the hindrance to the orientational disorder.[3−41]

One of the most interesting problems in relation to the OD phases arises as a consequence of the interplay between the molecular point-group symmetry and the usually high-symmetry crystal lattices. Usually the point-group symmetry of the molecule is lower than the lattice space group, thus forcing molecular reorientations along, at least, different axes. Early symmetry and steric considerations were used to derive the thermodynamic properties of phase transitions in these materials by Guthrie and McCullough,[5] assuming a number of distinguishable orientations in the OD phases, although the method was hardly questioned.[3,4,6] Many thermodynamic models (for a recent review see ref 42) extended the Lennard-Jones and Devonshire theory[43] by considering, as the key initial parameter, the number of permitted orientations of the molecular entity to rationalize the thermodynamic properties, with the pioneer being that of Pople and Karasz.[44,45] Nevertheless, despite the large molecular symmetry similarities, the polymorphic behavior of these *tert*-butyl materials has not been rationalized. Thus, out of necessity, particular characterization of each material is needed to compile similarities and differences which enable a possible overall description.

As for the *tert*-butyl bromide dealt with in this paper, polymorphism has been the subject of an intensive work.[3,14,19−22,24,26,28,30−35,37] It exists in three solid phases, designated I, II, and III in order of decreasing temperature and is one of the compounds possessing two stable OD phases (I and II). OD phase I is stable between ca. 232 K and the melting point (256 K), with the symmetry of the lattice being face-

* To whom correspondence should be addressed. E-mail: jose.luis.tamarit@upc.edu. Tel: +34 93 401 65 64. Fax: +34 93 401 18 39.
[†] Universitat Politècnica de Catalunya.
[‡] University of Augsburg.
[§] CNRS-Université Bordeaux I.

10.1021/jp061484+ CCC: $33.50
Published on Web 05/24/2006

centered cubic (FCC) with $Z = 4$. OD phase II transforms at 209 K to phase III.

The dynamical aspects of the polymorphism of this substance have been largely explored.[14,19,21−23,25,36] On the approach of the III to II transition, the rotation of the molecule about its 3-fold axis (C'_3) combined with internal rotation of the methyl groups (C_3) progressively develops. The dominating motion in phase II changes from C_3' reorientations in the low-temperature region to overall molecular tumbling in the high-temperature region.[19,23,25] In addition, incoherent quasielastic neutron-scattering experiments have shown phase II motions consisting of fluctuations of the dipolar axis[19] of about 30−60°, much greater than those for the molecular homologous *tert*-butyl chloride for which fluctuations cover only some degrees.[36] The results are consistent with the high values of the dielectric permittivity from dielectric measurements.[14,26] The birefringence of the uniaxial crystals of phase II was found early[27] and lately measured.[28] As a proof of the orientational disorder of the dipolar axis, an orientational order parameter describing the average over fluctuations of the dipolar axis from a preferred orientation, defined as $S = (1/2)\langle 3\cos\vartheta - 1\rangle$, where ϑ stands for the angle between the 3-fold symmetry axis of the molecule and crystal optical axis, was found to vary between 0.038 at 231 K and 0.052 at 210 K[28] or 0.0031−0.0044 in the same temperature range.[21] Because such an order parameter is an index on the extent to which the distribution of preferred orientations determined by molecular and crystallographic symmetries is weighted by intermolecular forces along a particular axis, weakly anisotropic large fluctuations of the molecular symmetry axis between preferred orientations were confirmed to be present in this uniaxial phase.

It is worth noting that molecular dynamics calculations on the rough sphere model at the melting point predicted greater rotational freedom in the solid-phase I than in the liquid.[29] A simple comparison of the distance between molecular centers $(((2)^{1/2}/2)a \approx 6.2$ Å) and any reasonable hard sphere diameter (>7 Å) indicates that steric effects are important. This is a general statement for OD phases (as well as for liquid phases) and evidences that motions involving translational−rotational coupling are significant.[38,39]

Although the more studied *tert*-butyl compounds correspond to the *tert*-butyl halides, only the structure of the lowest-temperature ordered phases of X═CN and X═Cl have been determined.[19,30,40] As for phase I of $(CH_3)_3CBr$, single crystals were grown from the liquid by Schwartz et al.[27] and oscillations diagrams were indexed on the basis of the FCC unit cell. This result was confirmed by many other X-ray and neutron powder diffraction studies.[31−33] Nevertheless, as far as lattice symmetry of phase II is concerned, results obtained from different works do not agree with each other. Some authors indexed the powder diffraction pattern on the basis of an orthorhombic unit cell.[5,32,33] Only recently was Rudman[34] able to obtain a single crystal of phase II by cooling a single crystal of isotropic phase I (as Akimov et al.[28] did for measurements of birefringence) and to state that phase II displays a rhombohedral unit cell with $a =$ 15.087(13) Å, $\alpha = 89.19(7)°$. The same author also indicated some possible relationships between phases I and II confirming the structural similarity between this rhombohedral phase II of $(CH_3)_3CBr$ and phase Ib of CCl_4. According to this similarity, a number of $Z = 21$ molecules per unit cell was assigned. Nevertheless, it should be noticed that the thermodynamic behavior of the OD phases of CCl_4 is quite different.[8−13] Upon cooling from the liquid, it crystallizes to an OD phase Ia (FCC) and upon further cooling to another OD phase Ib (R). When cooling is limited such that Ia is formed, this phase Ia melts upon heating without passing back through phase Ib. When heated from phase Ib, a new melting point several degrees higher than that of phase Ia is obtained. Then, it implies that phase Ia is a monotropic phase with respect to the rhombohedral phase Ib.

In this paper, we evidence the structural similarity and, even, the existence of a isomorphism relationship (the isostructural relationship being thus included) between not only phase II of $(CH_3)_3CBr$ with phase Ib of CCl_4 but also the FCC phases, stable for $(CH_3)_3CBr$ and metastable for CCl_4, of both compounds. To do so, orientationally disordered mixed crystals are studied for the whole range of compositions as well as a function of temperature. As a result, the melting phase diagram of the system $(CH_3)_3CBr + CCl_4$ is carefully analyzed by means of (micro-) calorimetry and high-resolution X-ray power diffraction.

2. Experimental Section

The chemicals CCl_4 and $(CH_3)_3CBr$ with purity higher than 99% were obtained from Across and Fluka, respectively, and the compounds were used as such. The transition temperatures and enthalpy changes for the pure and mixed crystals were measured by means of a Perkin-Elmer DSC-7 differential scanning calorimeter equipped with a homemade low-temperature device. High-pressure stainless steel pans from Perkin-Elmer were used to prevent sample reactions with the container as well as to resist the high vapor pressure of the compounds. Heating and cooling rates of 2 $K\cdot min^{-1}$ and sample masses around 15 mg were used.

A differential isothermal microcalorimeter, specifically designed to avoid vaporization of the liquids involved, was used to measure the excess enthalpy in the liquid state at 298.15 K. The microcalorimeter (BCP from Arion) was fitted with an automatic injection homemade device. The sample cell (ca. 10 cm^3) contains the liquids to be mixed isolated from one to another by a membrane. Details have been described elsewhere.[46]

High-resolution X-ray powder diffraction measurements using the Debye−Scherrer geometry and transmission mode were performed with a horizontally mounted INEL cylindrical position-sensitive detector (CPS-120) made of 4096 channels (0.029° 2θ angular step).[47] Monochromatic Cu $K\alpha_1$ radiation was selected by means of an asymmetrically focusing incident-beam curved quartz monochromator. The generator power was set to 40 kV and 30 mA. Low-temperature measurements were performed with a liquid nitrogen 600 series Cryostream Cooler from Oxford Cryosystems.

External calibration using cubic-phase $Na_2Ca_3Al_2F_4$ was performed to convert channels to 2θ degrees by means of cubic spline fittings to correct the deviation from angular linearity in PSD.[48] The peak positions were determined by pseudo-Voigt fittings.

The sample was introduced into 0.3-mm-diameter Lindemann glass capillaries in the liquid state at room temperature and was rotated perpendicularly to the X-ray beam during data collection to improve averaging of the crystallites. Acquisition times were at least 60 min for standard measurements.

3. Results

3.1. Differential Scanning Calorimetry. Temperature-composition two-phase equilibria involving OD and liquid phases corresponding to $[CCl_4]_{1-X}[(CH_3)_3CBr]_X$ mixed crystals have been obtained from DSC measurements.

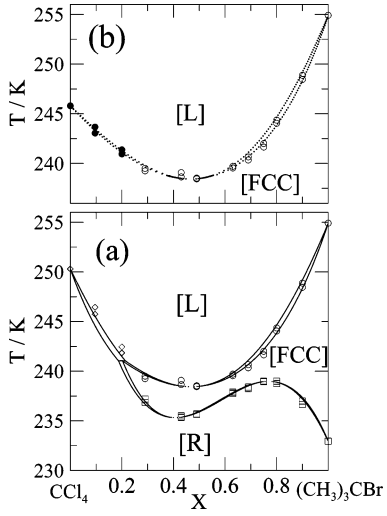

Figure 1. Temperature−composition CCl_4 + $(CH_3)_3CBr$ phase diagram. (a) Stable parts of the [R + L], [FCC + L], and [R + FCC] equilibria. (b) Metastable (full symbols) and stable (empty symbols) parts of the [FCC + L] equilibrium. Dashed curves correspond to the calculated phase equilibria obtained by the thermodynamic assessment.

The sample, any of given composition X, was cooled from room temperature to about 160 K at 2 K·min^{-1} and heated back to room temperature. Then the sample was cooled again until the first exothermic peak was recorded, that is, until the crystallization had occurred. Afterward, the so-obtained crystalline phase was heated to room temperature.

The behavior of the mixed crystals can be classified into two different composition ranges. For samples within the $0 \leq X \leq 0.20$ composition range, two phase transitions involving OD phases occur upon cooling while only one occurs upon heating back to room temperature. The X-ray diffraction measurements show that the previous sequence upon cooling is related to liquid−FCC and FCC−R phase transitions. The R mixed crystals do not revert to the FCC mixed crystals upon heating back and only the melting of the R phase is found. When cooling is limited such that the FCC phase is formed, this phase melts upon heating without transformation to the R phase. Then, the same monotropic behavior between R and FCC phases as for CCl_4 is found for this composition range.

For molar compositions higher than 0.20, the phase transitions appearing upon cooling are liquid to FCC and FCC to R, with all of them being reversible transitions. This evidences the enantiotropic relation between both OD phases in this composition range.

The stable $T-X$ diagram built up from the DSC and XRD experiments is plotted in Figure 1. The two-component system displays a peritectic three-phase equilibrium at 241 K sharing FCC, R, and L phases. As an uncommon feature, two extremes, minimum and maximum, are exhibited at the [R + FCC] equilibrium.

As can be seen from Figure 1, the two-phase equilibrium [FCC + L] goes continuously from $X = 0$ to $X = 1$, being stable from $X = 0.2$ to $X = 1$ and metastable from $X = 0$ to $X \approx 0.2$ (due to the monotropic behavior of the FCC phase). It is to be noticed that with decreasing mole fraction the [FCC + L] loop ends (at $X = 0$) at the FCC melting temperature of the CCl_4 pure component.

The heat effects associated with the solid−liquid and solid−solid phase transitions, derived from the DSC measurements, are depicted in Figure 2. It is worthwhile to mention that the enthalpy changes associated with the melting of the FCC mixed crystals could be measured continuously for the whole composition range and ought to be the real appearance of the metastable extension of the [FCC + L] equilibrium. Assuming that the specific heat of the OD FCC and R phases are close and due to the closeness of the melting temperatures of both OD mixed crystals, the enthalpy changes are combined by the equation

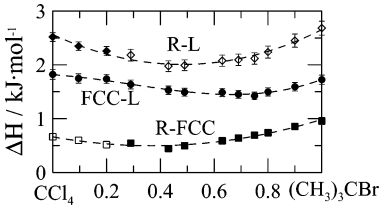

Figure 2. Experimental (full symbols) enthalpies of melting for the R (◆) and FCC (●) and for the R to FCC (■) transition as a function of the mole fraction. Empty symbols (◇,□) correspond to the calculated values from eq 1.

$$\Delta H_{R\rightarrow L} = \Delta H_{R\rightarrow FCC} + \Delta H_{FCC\rightarrow L} \quad (1)$$

From this equation, the melting enthalpy for the R mixed crystals for mole fractions higher than 0.2 (nonavailable experimentally) can be obtained (see Table 1). Extrapolation at $X = 1$ of the R to L melting enthalpy values enables us to obtain the enthalpy change associated with the (virtual) melting of the R phase of $(CH_3)_3CBr$. In addition, by use of the same procedure, the R to FCC enthalpy change can be calculated for samples for which this transition does not make a real appearance ($0 \leq X < 0.2$). It should be emphasized that extrapolation at $X = 0$ of the R to FCC enthalpy values or the value calculated from eq 1 virtually gives the same value for ΔH^{R-FCC} of CCl_4 (0.664 and 0.695 kJ·mol^{-1}, respectively) taking into account the experimental error limits. The same degree of agreement is found for the virtual melting enthalpy of the R phase of $(CH_3)_3CBr$ (using values generated by eq 1 for $0.2 < X < 1$) when comparing the value obtained from extrapolation at $X = 1$ for the R to L values (2.65 kJ·mol^{-1}) with that obtained from eq 1 (2.68 kJ·mol^{-1}). These values play a relevant role for the thermodynamic analysis, developed later in this work, which evidences the coherence of the experimental data.

As for the excess properties in the liquid state, we have measured the excess enthalpy of the liquid state at 298.2 K by using the mixing calorimeter. Figure 3 shows the obtained excess enthalpy.

3.2. Crystallographic Characterization of the Mixed Crystals. The isomorphic character of the OD FCC phases (metastable for CCl_4 and stable for $(CH_3)_3CBr$)) was shown by determining the lattice parameters as a function of composition from slowly cooling the liquid samples at 231.2 K. Results for the lattice parameter are shown in Figure 4a. The continuous variation of the lattice parameter vs composition proves the isomorphism relationship between both phases. Results for the pure compound $(CH_3)_3CBr$ ($a = 8.757(10)$ Å at 231.2 K) are in agreement with previously published data ($a = 8.79(2)$ Å at 243 K,[32] $a = 8.760(4)$ Å at 245 K.[34]).

As for the stable R mixed crystals, samples were cooled to the low-temperature phase and heated again up to 231.2 K. Figure 5 depicts a 2θ window of the diffraction patterns at 231.2 K for pure components and some representative mixed crystals. The close similarity between all of them evidences the existence of continuous formation of rhombohedral mixed crystals. Moreover, such an experimental result enables us to index the pattern of the R phase of $(CH_3)_3CBr$ and, thus, to confirm the lattice symmetry of such a phase II found recently by Rudman,[34] discarding then previous published symmetries.[32,33,35]

TABLE 1: Temperatures, Enthalpy, and Entropy Changes Associated with the Phase Transitions of CCl_4 and $(CH_3)_3CBr$ Obtained in This Work and from Previously Reported Adiabatic Calorimetry[a]

	transition	T/K	ΔH/kJ·mol^{-1}	ΔS/J·mol^{-1}·K^{-1}	ref
CCl_4	$M^S \rightarrow R^S$ [b]	225.9	4.68	20.72	this work
		225.35	4.581	20.33	49
		225.70 ± 0.01	4.631 ± 0.020	20.52	50
	$R^S \rightarrow L^S$	250.3	2.52	10.06	this work
		250.3	2.515	10.05	49
		250.53 ± 0.01	2.562	10.23	50
	$FCC^m \rightarrow L^m$	245.8	1.82	7.42	this work
		246.01 ± 0.01	1.830 ± 0.070	7.44	50
	$R^m \rightarrow FCC^m$	258.0†	0.66†	2.57†	this work
		262.9	0.69	2.64	12
$(CH_3)_3CBr$	$LT^S \rightarrow R^S$ [b]	209.0	5.90	28.2	this work
		209.4	5.85	27.2	24
		208.7	5.65	31	
	$R^S \rightarrow FCC^S$ [b]	232.9	0.96	4.11	this work
		231.9	0.97	4.5	24
		231.5	1.046	31	
	$FCC^S \rightarrow L^S$	254.9	1.72	6.77	this work
		256	1.966	7.5	41
		256.2	7.6	31	
	$R^m \rightarrow L^m$	246.5[c]	2.68[c]	10.88[c]	this work
			2.65[d]		this work

[a] The stable and metastable transitions are denoted by superscripts (s) and (m), respectively. [b] M refers to the low-temperature monoclinic ($C2/c$) phase of CCl_4, LT to that of $(CH_3)_3CBr$, and R and FCC for the OD phases. [c] Values obtained from fundamental thermodynamics (see text)‡. [d] Values obtained from the extrapolation of experimental values†.

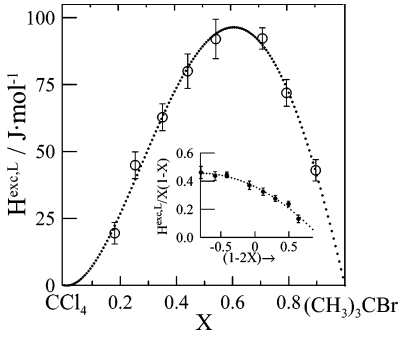

Figure 3. Experimental excess enthalpy, in the liquid state of binary mixtures of the $CCl_4 + (CH_3)_3CBr$ system at 293.2 K. The inset evidences the necessity of a three-parameter of a Redlich−Kister polynomial: $H^{exc,L}(X,T = 298.15\ K)/X(1 - X) = 358(10) - 231(14)\text{-}(1 - 2X) - 122(34)(1 - 2X)^2$ J·mol^{-1}.

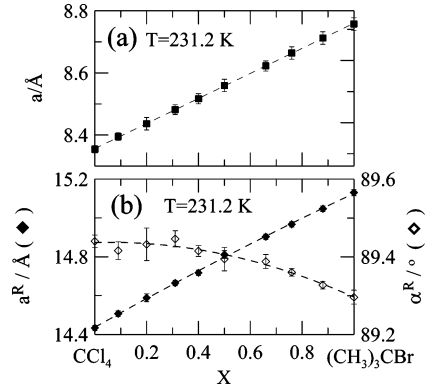

Figure 4. Lattice parameters for the FCC (a) and for the R (b) mixed crystals as a function of the mole fraction at 231.2 K.

Figure 6 shows the high-resolution X-ray diffraction pattern together with the FullProf fit of the R phase for $(CH_3)_3CBr$ at 215.0 K along with the difference profile. The obtained lattice parameters, $a^R = 15.068(7)$ Å and $\alpha^R = 89.29(1)°$, are in agreement with previous single-crystal results.[34] In Table 2, we compile the observed and calculated lattice spacings indexed according to this work as well as the observed neutron powder

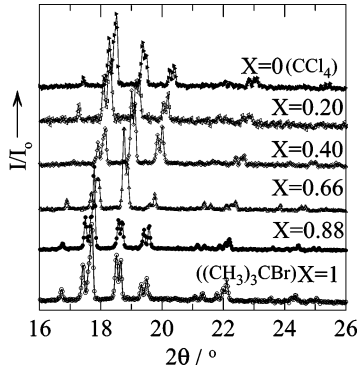

Figure 5. 2θ enlargement of the high-resolution X-ray powder diffraction patterns at 231.2 K of rhombohedral phase of pure components $(CH_3)_3CBr$ (lower trace) and CCl_4 (upper trace) and several mixed crystals.

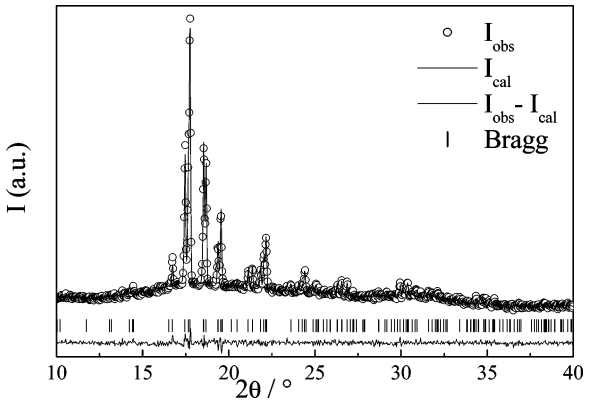

Figure 6. Observed X-ray diffraction pattern (circles) and FULLPROF fit (smooth curve) of the rhombohedral phase for $(CH_3)_3CBr$ at 215.0 K along with the difference profile (bottom line). The verticals bars stand for the Bragg reflections.

diffraction data collected by Ward[33] indexed as published in ref 34 (all of them at 215.0 K).

It should be noticed that indexing of high-resolution X-ray diffraction patterns by using standard procedures as Dicvol91[51]

TABLE 2: Experimental (d_{exp}) and Calculated (d_{cal}) Lattice Spacings (in angstroms) for the Reflections (hkl) of the OD Rhombohedral Phase of $(CH_3)_3CBr$ at 215.0 K Together with Values of Neutron Diffraction Data Collected by Ward,[33] d_{exp}[33] and Indexed (hkl[34]) as Published by Rudman in ref 34

$h\ k\ l$	d_{exp}	d_{cal}	$d_{exp} - d_{cal}$	d_{exp}[33]	$h\ k\ l$[34]
2 −1 1	6.1293	6.1383	−0.0089		
−2 2 0	5.2923	5.2944	−0.0021	5.293	2 2 0
					−2 2 0
2 2 1	5.0747	5.0777	−0.0029	5.068	2 2 1
					3 0 0
3 0 0	5.0155	5.0221	−0.0066		
−2 2 1	4.9911	4.9950	−0.0039	4.995	2 2 −1
					−2 2 1
3 1 0	4.7797	4.7820	−0.0023	4.801	3 1 0
−3 1 0	4.7452	4.7470	−0.0018	4.756	−3 1 0
3 1 1	4.5780	4.5785	−0.0005	4.572	3 1 1
3 −1 1	4.5386	4.5376	0.0009	4.527	−3 1 1
					3 −1 1
3 0 2	4.2005	4.2025	−0.0019		
3 −2 0	4.1562	4.1552	0.0010		
3 2 1	4.0652	4.0660	−0.0008	4.057	3 2 1
					3 2 −1
3 2 −1	4.0297	4.0302	−0.0005		
3 −2 1	4.0071	4.0022	0.0048		
−3 2 1	4.0071	4.0091	−0.0021	4.007	3 −2 1
					−3 2 1
4 0 0	3.7685	3.7666	0.0019		
2 3 2	3.6985	3.6970	0.0015		
4 1 0	3.6645	3.6647	−0.0002		
4 −1 0	3.6428	3.6436	−0.0008		
4 0 2	3.3853	3.3856	−0.0002		
−4 0 2	3.3541	3.3526	0.0016		
4 2 1	3.3159	3.3149	0.0010		
4 3 1	2.9823	2.9816	0.0008		
5 1 0	2.9620	2.9617	0.0002	2.970	4 3 1
					5 1 0
−5 1 0	2.9488	2.9478	0.0010		
4 −3 1	2.9393	2.9396	−0.0003	2.937	−5 1 0
					4 −3 1
					−4 3 1
−4 3 1	2.9393	2.9372	0.0021		

as implemented in the FullProf suite[52] or Treor[53] fell short of indexing the R phase of $(CH_3)_3CBr$ because reflections are closely spaced and, thus, many of them overlap (see the vertical bars showing the possible reflections in Figure 6). Thus, the comparison with patterns of the well-known R phase of CCl_4 and the continuous variation found for the mixed crystals was the unique unambiguous method. The fact that this quite different approach leads to the same lattice symmetry of the single-crystal indexing shows the robustness of the result obtained.

Another interesting conclusion concerning the assumed number of molecules in the unit cell ($Z = 21$) can be added. By means of the lattice parameters for both the R and FCC phases measured at 231.2 K (see Figure 4), it can be concluded that volume variation at the R−FCC transition (at 231.5 K) assuming 21 and 4 molecules per unit cell, respectively, is 1.80 $cm^3 \cdot mol^{-1}$ which coincides with the value (1.80 $cm^3 \cdot mol^{-1}$) obtained in ref 26 from the pressure−temperature phase diagram.

4. Thermodynamic Assessment

To derive the excess properties of the OD phases involved and to verify the thermodynamic coherence of the experimental phase diagram, a thermodynamic assessment has been carried out. The applied method has been largely described,[7,8,10−13,54] and thus, we will restrict the description only to the fundamental equations which, in addition, enable the reader to identify the thermodynamic magnitudes used. In the first section, we present a scheme for the derivation of equations, and in the second one, the thermodynamic properties derived for the two-component system are presented.

4.1. Thermodynamic Background. As a function of temperature T, the Gibbs energy function for a mixture of $(1 - X)$ moles of A and X moles of B in phase α reads

$$G^{\alpha}(T,X) = (1 - X)G_A^{*,\alpha} + XG_B^{*,\alpha} + RT[(1 - X)\ln(1 - X) + X \ln X] + G^{E,\alpha}(T,X) \quad (2)$$

where $G_i^{*,\alpha}$, i = A,B stands for the molar Gibbs energy of pure component i, R is the gas constant, and $G^{E,\alpha}(T,X)$ is the excess Gibbs energy, the deviation from the ideal mixing behavior. The two-phase equilibrium region between the liquid (L) and the α phase will be determined by the intersection between the Gibbs energies of both phases. Assuming that the specific heat does not change noticeably with temperature, it follows that

$$\Delta_{\alpha}^{L}G_i^*(T) = G_i^{*,L}(T) - G_i^{*,\alpha}(T) \approx \Delta_{\alpha}^{L}S_i^*(T_i^{\alpha\rightarrow L} - T) \quad (3)$$

where $\Delta_{\alpha}^{L}S_i^*$ is the melting entropy of the α phase at $T_i^{\alpha\rightarrow L}$, the equation

$$\Delta_{\alpha}^{L}G(T_{EGC},X) = 0 \quad (4)$$

provides a curve for equal values of the Gibbs energies of the α and L phases in the $T-X$ plane. The equation for this so-called equal-G curve (EGC)[54] is

$$T_{EGC}(X) = \frac{(1 - X)\Delta_{\alpha}^{L}H_A^* + X\Delta_{\alpha}^{L}H_B^*}{(1 - X)\Delta_{\alpha}^{L}S_A^* + X\Delta_{\alpha}^{L}S_B^*} + \frac{\Delta_{\alpha}^{L}G^{E}(X_{EGC})}{(1 - X)\Delta_{\alpha}^{L}S_A^* + X\Delta_{\alpha}^{L}S_B^*} \quad (5)$$

in which $\Delta_{\alpha}^{L}H_i^*$ is the melting enthalpy for component i and

$$\Delta_{\alpha}^{L}G^{E}(X_{EGC}) = G^{E,L}(T_{EGC},X_{EGC}) - G^{E,\alpha}(T_{EGC},X_{EGC}) \quad (6)$$

As the EGC is running between the solidus and liquidus curves of the [α + L] equilibrium, the estimated position of the EGC curve from the experimental data enables us, as follows from eq 4, to determine the excess Gibbs difference $\Delta_{\alpha}^{L}G_{EGC}^{E}(X)$ between the α and L phases. The EGC method (also known as Oonk's method[54]) is applied by means of the WINIFIT[55] or LIQFIT[56] programs. It should be stressed that in the present melting equilibria ([R + L] and [FCC + L]) the temperature range of the phenomena is rather small, and thus, we can express the excess Gibbs energies as a temperature-independent Redlich−Kister j-order polynomials

$$G^{E,\alpha}(X) = X(1 - X)[\sum_{j=1} G_j^{\alpha}(1 - 2X)^{j-1}] \quad (7)$$

4.2. Thermodynamic Assessment of the Equilibria. Table 1 gathers the temperatures and enthalpy changes corresponding to the melting of the stable and metastable OD phases of the pure compounds.

As for the [FCC + L] loop, it must be noticed that the metastable FCC melting of the CCl_4 component as well as the melting of the mixed crystals for the whole range of mole fraction are experimentally available. It means that thermodynamic assessment could be done with any additional hypothesis.

TABLE 3: Calculated Redlich−Kister Coefficients for the Excess Enthalpy and for the Excess Gibbs Energy Difference between FCC, R, and Liquid Phases in the $CCl_4 + (CH_3)_3CBr$ Two-component System

H^{exc} (J·mol^{-1})				$\Delta_\alpha^\beta G^{exc} = G^{exc,\beta} - G^{exc,\alpha}$ (J·mol^{-1})				
	H_1	H_2	H_3	β	α	ΔG_1	ΔG_2	ΔG_3
R	2562	−619	−627	L	R	−449	−174	36
FCC	1402	−873	−491	L	FCC	−331	73	
L	358	−231	−122	R	FCC	118	247	−36

Table 3 summarized the results for the determined Redlich−Kister coefficients, and Figure 1 shows the calculated loop, which fully agrees with the experimental data.

For the [R + L] loop, only the stable part can be measured, so that its metastable extension ends in the theoretical melting point of the R phase of the $(CH_3)_3CBr$ compound. As the stable [R + L] loop extends to a maximum of about 20% of the mole fraction scale (see Figure 1), extrapolating the liquidus to $X = 1$, that is, $(CH_3)_3CBr$, would lead to a significant error for the melting temperature $T_m^{R\rightarrow L}$ of $(CH_3)_3CBr$.

We have performed then an assessment of the [R + FCC] loop. In this case, the thermodynamic properties of the R to FCC metastable transition of CCl_4 have been determined by extrapolation, with its values being consigned in Table 1. After the thermodynamic excess Gibbs energy difference from the aforementioned two-phase equilibria was determined, complete calculation of the melting phase diagram can be done. Figure 1 details the almost perfect agreement with the experimental data.

To emphasize the agreement between calculated equilibria and the experimental values, we have analyzed the singularities of the equilibria. These singularities make their appearance in Figure 7, in which the Gibbs energy difference $G^{FCC} - G^R$-(T,X) is displayed at several relevant temperatures: peritectic temperature [R + FCC + L], as well as the temperature at which the [R + FCC] loop displays maximum and minimum extremes. This is really one of the very few systems showing a solid−solid equilibrium with such extremes.

A similar analysis for the melting loops provides the temperature and composition of the extremes (minima). As for the [FCC + L] loop values ($T = 238.45$ K, $X = 0.47$), they are in full agreement with the experimental data while those for the [R + L] ($T = 237.5$ K, $X = 0.44$) belong to the nonexperimentally available region of the loop.

An interesting point to emphasize the coherence of the derived excess functions concerns the excess enthalpy of the OD phases. With the excess enthalpy of the liquid phase obtained by means mixing calorimetry (Figure 3) and the melting enthalpies of the R and FCC mixed crystals, the excess enthalpies of both OD phases can be calculated by means of the equation

$$H^{exc,\alpha}(X) = (1 - X)\Delta_\alpha^L H_A^* + X\Delta_\alpha^L H_B^* - \Delta_\alpha^L H(X) + H^{exc,L}(X), \quad \alpha = R,FCC \quad (8)$$

This equation embodies the assumption that the excess enthalpies are temperature-independent. Figure 8 displays the calculated excess enthalpy for the OD phases together with the experimental excess enthalpy of the liquid phase. To check the temperature-independent assumption, the calculated excess enthalpy difference between the OD phases, $\Delta_R^{FCC}H^{exc} = H^{exc,R} - H^{exc,FCC}$, is compared with the experimental values. Despite the very small values and the fact that a set of them was obtained by the difference of experimental heats of melting of the R and FCC mixed crystals, it is even remarkable how similar the calculated and experimental curves are.

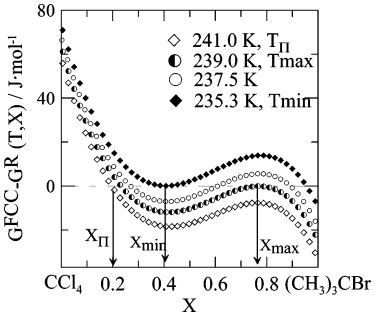

Figure 7. Gibbs energy difference between the FCC and R mixed crystals at some characteristic temperatures: (◇) $T_\Pi = 241.0$ K ($X_\Pi = 0.215$), the peritectic temperature (R + FCC + L), (◐) $T_{max} = 239.0$ K ($X_{max} = 0.770$) and (◆) $T_{min} = 235.3$ K ($X_{min} = 0.$ 0.405), the temperatures of the maximum and minimum Gibbs points for the [R + FCC] equilibrium, and (○) 237.5 K, an intermediate temperature between the Gibbs points. The mole fractions of the characteristic points are also shown.

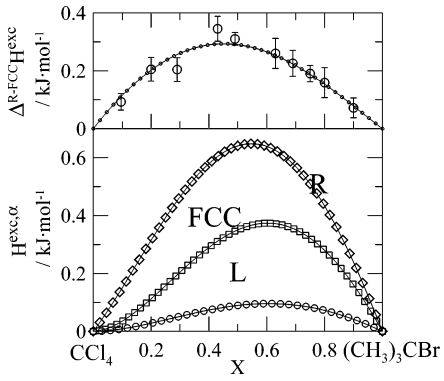

Figure 8. Excess enthalpies of the OD phases R and FCC derived from eq 8 (together with that of the liquid) (lower frame) and the excess enthalpy difference of the OD phases (upper frame).

5. Discussion and Conclusions

A recent uniform thermodynamic description of mixed crystals sharing methyl-chloromethane compounds, $(CH_3)_{4-n}CCl_n$, $n = 0,...,4$, in which R and FCC mixed crystals also made appearance, has shown that their excess properties are related to the volumetric mismatch between the components of a system, together with the dipolar nature of the shared molecules.[57] Thus, the equimolar excess enthalpy was parametrized by means of the "m" mismatch geometric parameter, defined as $m = |\Delta V|/V_m$, where $|\Delta V|$ is the difference between the molar volumes of the components and V_m their mean. For the system studied in this work, it appears the paradox of the m parameter is, within experimental error limits, virtually the same for both kinds of mixed crystals ($m^R = m^{FCC} = 0.141$). Moreover, according to that work, the system $CCl_4 + (CH_3)_3CBr$ would belong to the category of systems in which dipole dilution appears, that is, the system under scrutiny comprises a material devoid (CCl_4) and another ($(CH_3)_3CBr$) having a strong molecular dipole moment. The correlation for the binary systems sharing methyl-chloromethane compounds provided then an excess enthalpy for the R mixed crystals with $m^R = 0.141$ of $H^{exc,R}(X = 0.5) = 0.74 \pm 0.10$ kJ·mol^{-1}, which compares well with the value obtained in this work (0.64 ± 0.20 kJ·mol^{-1}). Although for the global correlation FCC mixed crystals were also involved, only a reduced number of mixed crystals with such symmetry was considered. It is difficult to assume that the correlation still remains for FCC mixed crystals, because the experimental value for the equimolar excess enthalpy,

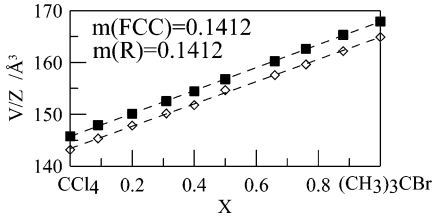

Figure 9. Volume occupied by a molecule for the R (◇) and FCC (■) mixed crystals as a function of composition at 231.2 K.

$H^{exc,FCC}(X = 0.5) = 0.35 \pm 0.10$ kJ·mol^{-1}, is clearly far away from the claimed value with $m^{FCC} = 0.141$ (again 0.74 ± 0.10 kJ·mol^{-1}).

Although for that correlation, additional experimental data is needed, and especially for FCC mixed crystals, it seems that deviation for the ideal behavior would strongly depend on the symmetry of the translational long-range order and not only on the volumetric properties and the dipolar character of the shared molecules. This would seem very surprising if one assumes that orientational disorder appears in both R and FCC phases. Nevertheless, we must bear in mind that strong orientational correlations can appear in OD phases (or even in the liquid phase) whatever the symmetry and whatever the dipolar character of the molecule.[38,39,58]

Noteworthy is the fact that both excess enthalpies are positive, which means that for both kinds of mixed crystals the attraction between the molecular entities A and B is weaker than the mean of the attractions A−A and B−B in pure components, giving then rise to a net repulsion.

It is of interest to note that the FCC lattice parameter as a function of composition changes from 8.354(6) Å (CCl_4) to 8.757(10) Å ($(CH_3)_3CBr$) at 231.5 K, which implies a volume change along the whole composition range of about 15%. Such a change, which in addition is almost linear, goes along the molecular volume difference of the involved pure compounds, 87.72 and 101.07 A^3 for CCl_4 and $(CH_3)_3CBr$, respectively.[59] In other words, FCC and R mixed crystals seem to be built up, from a crystallographic point of view, purely by stearic considerations. Nevertheless, thermodynamic properties cannot be reasonably explained without taking into account additional physical effects (as short-range orientational correlations). Thus, while it has been clearly stated that excess enthalpies for FCC and R mixed crystals differ by more than 50% (at the equimolar composition), the similarity of the stearic effects in both OD mixed crystals as revealed by the similar dependence of the lattice volume variation against mole fraction (Figure 9) does not go along with the excess energetic properties. On the other hand, excess enthalpy functions for OD and liquid phases are monotonic functions (see Figure 8), without maxima or minima accounting for the singularities of the equilibrium loops (see Figure 1). Of special relevance in this point is the maximum and minimum for the [R + FCC] loop. As evidenced by Figure 7, the Gibbs energy difference between FCC and R mixed crystals reveals several singularities which are not present in the excess enthalpy functions. The combination of $G^{exc,\alpha}$ for given T, and $H^{exc,\alpha}$ gives $S^{exc,\alpha}$ by the relation $G^{exc,\alpha} = H^{exc,\alpha} - T \cdot S^{exc,\alpha}$. Because of the lack of data for $G^{exc,L}$ (typically derived from isothermal liquid−vapor equilibria), excess entropy functions for the OD phases cannot be derived. Nevertheless, without consideration of the specific dependence on the mole fraction for each excess entropy function, details not only on the excess entropy but also on the changes of the configurational entropy as a function of temperature and mole fraction would provide enormous insights into the short-range orientational order, which in turn, would bring evidences on the differences between the local order of the OD and liquid phases.[60−63]

Acknowledgment. The research was supported by the Spanish Ministry of Education and Science under Project FIS2005-00975 and by the government of Catalonia under Project 2005SGR-00535.

References and Notes

(1) Sherwood, J. N. *The Plastically Crystalline State*; Wiley: New York, 1979.
(2) Parsonage, N. G.; Staveley, L. A. K. *Disorder in crystals*; Clarendon Press: Oxford, U.K., 1978.
(3) Reuter, J.; Büsing, D.; Tamarit, J. Ll.; Würflinger A. *J. Mater. Chem.* **1997**, *7*, 41.
(4) Jenau, M.; Reuter, J.; Würflinger, A.; Tamarit, J. Ll. *J. Chem. Soc. Faraday Trans.* **1996**, *92*, 1899.
(5) Guthrie, G. B.; McCollough, J. P. *J. Phys. Chem. Solids* **1961**, *18*, 53.
(6) Clark, T.; McKervey, M. A.; Mackle, H.; Rooney, J. J. *J. Chem. Soc., Faraday Trans. 1* **1974**, *7*, 1279.
(7) Pardo, L. C.; Barrio, M.; Tamarit, J. Ll.; Negrier, P.; López, D. O.; Salud, J.; Mondieig, D. *J. Phys. Chem. B* **2001**, *105*, 10326.
(8) Pardo, L. C.; Barrio, M.; Tamarit, J. Ll.; López, D. O.; Salud, J.; Negrier, P.; Mondieig, D. *Phys. Chem. Chem. Phys.* **2001**, *3*, 2644.
(9) Rudman, R.; Post, B. *Science* **1966**, *154*, 1009.
(10) Pardo, L. C.; Barrio, M.; Tamarit, J. Ll.; López, D. O.; Salud, J.; Negrier, P.; Mondieig, D. *Chem. Phys. Lett.* **1999**, *308*, 204.
(11) Pardo, L. C.; Barrio, M.; Tamarit, J. Ll.; López, D. O.; Salud, J.; Negrier, P.; Mondieig, D. *Chem. Phys. Lett.* **2000**, *321*, 438.
(12) Pardo, L. C.; Barrio, M.; Tamarit, J. Ll.; Negrier, P.; López, D. O.; Salud, J.; Mondieig, D. *J. Phys. Chem. B* **2004**, *108*, 11089.
(13) Pardo, L. C.; Barrio, M.; Tamarit, J. Ll.; López, D. O.; Salud, J.; Negrier, P.; Mondieig, D. *Chem. Phys. Lett.* **2002**, *355*, 339.
(14) Richardson, R. M.; Taylor, P. *Mol. Phys.* **1984**, *3*, 525.
(15) Hasebe, T. *Bull. Chem. Soc. Jpn.* **1990**, *63*, 2877
(16) Chen, J.; Bartell, L. S. *J. Phys. Chem.* **1993**, *97*, 10645.
(17) Ferrrario, M.; McDonald, I. R. *J. Chem. Phys.* **1985**, *83*, 4726.
(18) Ward, R. C.; Leadbetter, A. J.; Richardson, R. M.; Stirling, W. G. *Mol. Phys.* **1987**, *60*, 213.
(19) Leadbetter, A. J.; Ward, R. C.; Richardson, R. M. *J. Chem. Soc. Faraday Trans. 2* **1985**, *81*, 1067.
(20) ; Strange, J. H.; Nakamura, N.; Chihara, H. *J. Chem. Soc. Faraday Trans. 2* **1985**, *81*, 749.
(21) Pettitt, B. A.; Lewis, J. S.; Wasylishen, R. E.; Danchura, W.; Tomchuk, E. *J. Magn. Reson.* **1981**, *44*, 508.
(22) Ferrario, M.; Klein, M. L.; Lynden-Bell, R. M.; McDonald, I. R. *J. Chem. Soc., Faraday Trans. 2* **1987**, *83*, 2097.
(23) Hasebe, T.; Strange, J. H. *J. Chem. Soc., Faraday Trans. 2* **1985**, *84*, 187.
(24) Wenzel, U.; Schneider, G. M. *Thermochim. Acta* **1986**, *109*, 111.
(25) Aksnes, D. W.; Ramstad, K.; Björlykke, O. P. *Magn. Reson. Chem.* **1987**, *25*, 1063.
(26) Kreul, H.-G.; Hartmann, M.; Edelmann, R.; Würflinger, A. *Ber. Bunsen-Ges. Phys. Chem.* **1989**, *93*, 612.
(27) Schwartz, R. S.; Post, B.; Fankuchen, I. *J. Am. Chem. Soc.* **1951**, *73*, 4490.
(28) Akimov M. N.; Bezrukov, O. F.; Vuks, M. F., Struts, A. V. *Mol. Cryst. Liq. Cryst.* **1990**, *192*, 97.
(29) O'Dell, J.; Berne, J. *J. Chem. Phys.* **1975**, *63*, 2376.
(30) Rudman, R. *J. Mol. Struct.* **1999**, *485*, 281
(31) Urban, S. *Adv. Mol. Relax. Interact. Processes* **1981**, *21*, 221.
(32) Urban, S.; Domoslawski, J.; Tomkowicz. *Mater. Sci.* **1978**, *4*, 91.
(33) Ward, R. C. Neutron Scattering from Orientationally Disordered Crystals. Thesis, University of Exeter, Exeter, U.K., 1982.
(34) Rudman, R. *J. Mol. Struct.* **2001**, *569*, 157.
(35) Bertie, J. E.; Sunder, S. *Spectrochim. Acta, Part A* **1974**, *30*, 1373.
(36) Hasebe, T.; Ohtani, S. *J. Chem. Soc., Faraday Trans. 1* **1988**, *84*, 187.
(37) Bertie, J. E.; Sunder, S. *J. Chem. Phys.* **1973**, *59*, 498.
(38) Pardo, L. C.; Veglio, N.; Bermejo, F. J.; Tamarit, J. Ll.; Cuello, G. J. *Phys. Rev. B* **2005**, *72*, 014206.
(39) Veglio, N.; Bermejo, F. J.; Pardo, L. C.; Tamarit, J. Ll.; Cuello, G. J. *Phys. Rev. E* **2005**, *72*, 031502.
(40) Tamarit, J. Ll.; López, D. O.; Alcobé, X.; Barrio, M.; Salud, J.; Pardo, L. C. *Chem. Mater.* **2000**, *12*, 555.
(41) Kushner, L. M.; Crowe, R. W.; Smith, C. P. *J. Am. Chem. Soc.* **1951**, *73*, 4490.
(42) Özgan, S.; Demirkol, I. *Physica B* **2005**, *364*, 311.
(43) Lennard-Jones, J. E.; Devonshire, A. F. *Proc. R. Soc.* **1939**, *169*, 317.
(44) Pople, J. A.; Karasz, F. E. *J. Phys. Chem. Solids* **1961**, *18*, 28.

(45) Karasz, F. E.; Pople, J. A. *J. Phys. Chem. Solids* **1961**, *20*, 294.
(46) Rute, M. A.; Salud, J.; Negrier, P.; López, D. O.; Tamarit, J. Ll.; Puertas, R.; Barrio, M.; Mondieig, D. *J. Phys. Chem. B* **2003**, *107*, 5914.
(47) Ballon, J.; Comparat, V.; Pouxe, J. *Nucl. Instrum. Methods* **1983**, *217*, 213.
(48) Evain, M.; Deniard, P.; Jouanneaux, A.; Brec, R. *J. Appl. Crystallogr.* **1993**, *26*, 563.
(49) Morrison, J. A.; Richards, E. L.; Sakon, M. *J. Chem. Thermodyn.* **1976**, *8*, 1033.
(50) Hicks, J.; Hooley, J.; Stephenson, J. G. *J. Am. Chem. Soc.* **1944**, *66*, 1064.
(51) Boultif, A.; Louër, D. *J. Appl. Crystallogr.* **1991**, *24*, 987.
(52) Rodriguez-Carvajal, J.; Roisnel, T.; Gonzales-Platas, J. *FullProf Suite* (April 2004 version); Laboratoire Léon Brillouin, CEA-CNRS, CEN Saclay, France.
(53) Werner, P. E.; Eriksonn, L.; Westdahl, M. *J. Appl. Crystallogr.* **1985**, *18*, 367.
(54) Oonk, H. A. J. *Phase Theory*: *The Thermodynamics of Hetereogeneous Equilibria*; Elsevier Science Publishers: Amsterdam, The Netherlands, 1981.
(55) Daranas, D.; López, R.; López, D. O. *WINIFIT 2.0*.; Technical University of Catalonia: Catalonia, Spain, 2000 (available on http://fisicaetseib.upc.es/lcm/).
(56) Jacobs, M. H. G.; Oonk, H. A. J. *LIQFIT. A computer program for the Thermodynamic Assessment of T−X Liquidus or Solidus Data*; Utrecht University: Utrecht, The Netherlands, 1990.
(57) Pardo, L. C.; Barrio, M.; Tamarit, J. Ll.; López, D. O.; Salud; Oonk, H. A. J. *Chem. Mater.* **2005**, *17*, 6146.
(58) Egelstaff, P. A.; Page, D. I.; Powles, J. G. *Mol. Phys.* **1971**, *20*, 881.
(59) Bond lengths and van der Waals radii were taken from A. Kitaigorodsky, ''*Organic Chemical Crystallography"* Consultants, Bureau: New York, 1961.
(60) Bagchi, B.; Chandra, A. *Phys. Rev. Lett.* **1990**, *64*, 455.
(61) Price, D. L.; Saboungi, M. L.; Bermejo, F. J. *Rep. Prog. Phys.* **2003**, *66*, 407.
(62) Criado, A.; Jiménez-Ruiz, M.; Cabrillo, C.; Bermejo, F. J.; Fernández-Perea, R.; Fischer, H. E.; Trouw, F. R. *Phys. Rev. B* **2000**, *61*, 12082.
(63) Jedlovszky, P. *J. Chem. Phys.* **1997,** *107*, 7433.